

The Inner Scale Length of Spiral Galaxy Rotation Curves

Riccardo Giovanelli, Martha P. Haynes

Center for Radiophysics and Space Research and National Astronomy and Ionosphere Center ¹,
 Space Sciences Bldg., Cornell University, Ithaca, NY 14853
e-mail: riccardo@astro.cornell.edu, haynes@astro.cornell.edu

ABSTRACT

We use the tapering effect of $H\alpha/[N\ II]$ rotation curves of spiral galaxies first noted by Goad & Roberts (1981) to investigate the internal extinction in disks. The scale length of exponential fits to the inner part of rotation curves depends strongly on the disk axial ratio. Preliminary modelling of the effect implies substantial opacity of the central parts of disks at a wavelength of $0.66\ \mu$. In addition, the average kinematic scale length of rotation curves, when corrected to face-on perspective, has a nearly constant value of about $1.7h^{-1}$ kpc, for all luminosity classes. The interpretation of that effect, as the result of the increasing dominance of the baryonic mass in the inner parts of galaxies, yields a mean baryonic mass-to-light ratio in the I band $\tilde{T}_I = 2.7h\ M_{\odot}/L_{\odot,I}$, within the inner $1.7h^{-1}$ kpc of disks.

Subject headings: galaxies: spiral; photometry; fundamental parameters; halos – ISM: dust, extinction

1. Introduction

At optical and near infrared wavelengths, interstellar dust depresses the observed flux of galaxy disks by both scattering and absorption. Several authors have proposed that, even in the face-on perspective, normal, non-starburst disks are optically thick at optical wavelengths, while others have argued for substantial transparency (see the volume edited by Davies & Burstein 1995 and the review by Calzetti 2001 for details). Using a sample of spiral galaxies within $cz \sim 10,000\ \text{km s}^{-1}$, we statistically derived photometric solutions for the degree of internal extinction at I-band as a function of disk inclination (Giovanelli *et al.* 1994), finding a difference of more than a magnitude of flux between face-on and edge-on systems. At the same time, we found evidence for transparency of the outer parts of disks, at radii > 3 disk scale lengths from the center. We later reported that the amount of internal extinction is luminosity dependent: more luminous disks being more opaque

¹The National Astronomy and Ionosphere Center is operated by Cornell University under a cooperative agreement with the National Science Foundation.

than less luminous ones (Giovanelli *et al.* 1995). These results have been confirmed by more recent analyses (e.g. Tully *et al.* 1998; Wang & Heckman 1996).

Purely photometric techniques are subject to a peculiar set of selection effects, that can severely affect quantitative conclusions on internal extinction, as witnessed by the liveliness of the debate over the last decade. In 1981, Goad & Roberts noted a kinematic effect which can provide an independent test for disk extinction.

Let $V(r)$ be the rotation curve of a disk (r being the radial coordinate along the disk’s projected major axis), assumed to have axial symmetry. Let (x, y) be a set of Cartesian coordinates *in the plane of the disk*. If the disk is thin and it is observed at inclination i ($i = 90^\circ$ for edge-on), the component of velocity along the line of sight which intercepts the disk at (x, y) is

$$V_{\parallel} = V(r) \frac{x}{\sqrt{x^2 + y^2}} \sin i + V_{turb}, \quad (1)$$

where V_{turb} accounts for turbulence and x is oriented along the disk’s apparent major axis. An observed rotation curve, as derived for example from a long-slit $H\alpha$ spectrum positioned along x , is smeared by seeing, instrumental resolution, averaging across the slit width, the finite thickness of the disk and extinction occurring within the disk itself. As realistically thick disks approach the edge-on perspective, lines-of-sight along the major axis sample regions of increasingly broad range in y , yielding a velocity distribution with a peak velocity contributed by parcels of gas at $y = 0$ and a low velocity wing contributed by parcels at $|y| > 0$. If extinction is important, only foreground parts of the disk contribute to the emission and the factor $(x/\sqrt{x^2 + y^2}) < 1$ depresses the velocity distribution observed at $r = x$. Goad & Roberts noted how this tapering effect may, in opaque edge-on disks, produce observed rotation curves resembling solid-body behavior, independently of the true shape of $V(r)$. Bosma *et al.* (1992) applied this technique to two edge-on systems, NGC 100 and NGC 891, by comparing HI synthesis and $H\alpha$ observations. The evidence led them to conclude that the disk of NGC 100 is transparent, while in the case of NGC 891 they could not exclude the possibility of extinction in the inner parts of the disk. Prada *et al.* (1994) compared long-slit spectra of NGC 2146 in the optical and near IR and reported evidence for extinction in the inner parts of the galaxy.

Here, we apply the Goad & Roberts test in a statistically convincing manner to a sample of more than 2000 $H\alpha/[N\ II]$ rotation curves. Our results clearly indicate substantial opacity in the inner disks of spiral disks. They also show the effect to be luminosity dependent, in a manner very much in agreement with our previous photometric determination. In Section 2 we present our data sample and describe our rotation curve fits. Results on extinction are discussed in Section 3. In Section 4, we discuss an interesting serendipitous finding: the apparent constancy of the mean value of the kinematic scale length of $H\alpha/[N\ II]$ rotation curves, across populations of different luminosity class. Throughout this paper, distances and luminosities are obtained from redshifts in the Cosmic Microwave Background reference frame and scaled according to a Hubble parameter $H_0 = 100h\ \text{km s}^{-1}\ \text{Mpc}^{-1}$.

2. Data Sample and Rotation Curve Model Fits

As an effort to map the peculiar velocity field of the local Universe, we have assembled a sample of several thousand observations of I-band photometry and rotational width data of spiral galaxies. Our observations, including those listed in Dale & Giovanelli (2000 and refs. therein) as well as several hundred obtained at the Hale 5 m telescope after that report and to be presented elsewhere, have been complemented by the samples observed in the southern hemisphere by Mathewson and co-workers (Mathewson *et al.* 1992; Mathewson & Ford 1996). The kinematic information for a substantial subset of these data is in the form of rotation curves in electronic form, derived from long-slit $H\alpha/[N II]$ spectra.

Rotation curves can be fitted by a variety of parametric models, some of which are motivated by the physical expectation of contributions by a baryonic component with a mass distribution mimicking that of the light plus a dark matter spheroidal halo. Other models rely purely on the versatility of a mathematical form in fitting effectively the observed rotation curves with a minimum of free parameters. Here we report on fits to 2246 rotation curves with a parametric model of the form

$$V_{pe}(r) = V_o(1 - e^{-r/r_{pe}})(1 + \alpha r/r_{pe}) \quad (2)$$

where V_o regulates the overall amplitude of the rotation curve, r_{pe} yields a scale length for the inner steep rise and α sets the slope of the slowly changing outer part. This simple model, which we refer to as *Polyex*, has been found to be very “plastic”. It fits effectively both the steeply rising inner parts of rotation curves, as well as varying outer slopes, and it can be used to advantage in estimating velocity widths at specific radial distances from the galactic center as required by applications of the luminosity–linewidth relation. In particular, it provides a very useful estimate of the inner slope of the rotation curve as given by r_{pe} . Of the 2246 rotation curves fitted by the model shown in Equation (2), 425 have been rejected due to poor quality of the data or of the fit or because r_{pe} projects to less than 3” and may thus be affected by poor angular resolution. Mean values of α , the value of r_{pe} as seen in face-on systems, r_{pe}^o , and of the ratio between r_{pe} and the scale length of the disk light for face-on systems are given in Table 1, for different luminosity bins; mean values of r_{pe} are shown in Figure 1 and discussed in the next section, where they are used to probe disk extinction. Contents of columns 5 and 6 of Table 1 are discussed in Section 4.

3. Evidence for Extinction

In Figure 1, the mean value of r_{pe} is shown separately for different luminosity classes, as a function of the disk inclination as expressed by $\log(a/b)$, where (a/b) is the apparent axial ratio. Each symbol is the average within a bin including between 20 and 30 galaxies. The horizontal dotted line in each panel indicates an arbitrary scale of $1.6h^{-1}$ kpc. The total number of galaxies and the absolute magnitude range is indicated within each panel of the Figure. The parameter r_{pe} gives an indication of the radial distance at which the rotational velocity is $1 - 1/e = 0.63$ of

$V_o(1 + \alpha)$ (the asymptotic velocity for flat rotation curves, for which $\alpha = 0$). Figure 1 shows that, as $\log(a/b)$ approaches 0.45 ($i \simeq 70^\circ$), the kinematic scale length r_{pe} of observed rotation curves starts increasing. The effect is more marked for more luminous disks, for which edge-on systems exhibit an average value of r_{pe} nearly three times as large as that of systems with $i < 45^\circ$. The effect is not evident in the least luminous systems (those with $M_I - 5 \log h$ fainter than -19.5). This result is in agreement with the expectations based on the photometric determination of Giovanelli *et al.* (1995). No axial ratio dependence is observed for α , the outer slope of the rotation curves.

We have carried out preliminary modelling of the observations shown in Figure 1 by simulating the dust and H α distributions as exponential disks both in r and z . Assuming the same distribution for dust and H α tracers, with a ratio between scale height and scale length of 0.06 (as found by Xilouris *et al.* 1997; 1998), we obtain approximate match between models and Figure 1 for values of the face-on ($i = 0^\circ$), central ($r = 0$) optical depth of the model at the wavelength of H α ($\lambda = 0.66\mu$), $\tau_\alpha^\circ(0)$, of about 4. These modelling results are preliminary and depend very sensitively on the assumed thickness of disks and on the relative scales of dust and H α sources. We will report more extensively on the results of this effort at a later stage.

4. A Characteristic Kinematic Scale Length

Figure 1 shows that, for low axial ratios (where the effect of internal extinction is negligible), the average value of the kinematical scale length r_{pe} is approximately the same for disks of all luminosities. Is this result to be expected?

First, we exclude that the angular resolution of spectroscopic observations has a significant impact on the reported findings. Not using galaxies for which r_{pe} projects to an angular size $a_{pe} < 3''$ rules out bias due to extreme cases of poor angular resolution. Since we use rotation curves from different sources, which have been produced with different angular sampling intervals, we have also verified that there is no systematic difference in the fitted values of a_{pe} among different data sources, taking advantage of significant sample overlaps. We have done so for several dozen galaxies appearing in at least two samples among those: of our own, of Mathewson *et al.*, of Courteau (1997) and of Rubin *et al.* (1999 and refs. therein).

Second, we explore the effect of sample selection criteria. The values of $\langle r_{pe} \rangle$ displayed in Figure 1 are affected by Malmquist bias, which does not impact on the trends produced by extinction but alters the relative values of $\langle r_{pe} \rangle$ among different luminosity classes: since more luminous populations have larger average distance, for them the angular size limit of $3''$ produces an $\langle r_{pe} \rangle$ biased high. In order to remove this bias, we draw a subsample which is volume limited, by including in it only systems with $a_{pe} > 3''$, $hr_{pe} > 1$ kpc and within the distance range $20h^{-1}$ to $80h^{-1}$ Mpc. At $80h^{-1}$ Mpc, an angular size limit of $3''$ translates into a linear size limit of about 1 kpc; the reason for a lower limit in distance is to reduce the uncertainty introduced by peculiar velocities. We further restrict the subsample to low inclination disks ($\log(a/b) < 0.3$,

< 0.4 , < 0.5 respectively for $M - 5 \log h < -21.0$, < -19.5 and > -19.5) — in order to get around the extinction effect discussed in the previous section — and compute the mean values of r_{pe} and a_{pe} , now identified by a subscript “1”; those values are listed in columns 5 and 6 of Table 1, for each luminosity class. The exclusion of galaxies with $hr_{pe} < 1$ kpc biases high the values of $< hr_{pe} >_1$; it does so however equally for all luminosity classes, through which $< hr_{pe} >_1$ remains approximately constant. The mean values $< a_{pe} >_1$, which increase with decreasing luminosity, illustrate the fact that less luminous populations are on the average more nearby. Note that the values of $< a_{pe} >_1$ are fairly large in comparison with the typical seeing, excluding the likelihood of an angular resolution bias.

Next, we inquire on the implications of a constant r_{pe} on the total mass distribution. Assume the total mass of the galaxy M_{200} is that comprised within a limiting radius r_{200} , defined as that within which the halo mean density is 200 times the critical density of the Universe. Then,

$$M(r_{pe}) = M_{200} \frac{\bar{\rho}(r_{pe})}{\bar{\rho}_{200}} \left(\frac{r_{pe}}{r_{200}} \right)^3 \quad (3)$$

where $M(r_{pe})$ is the mass within r_{pe} , and $\bar{\rho}(r_{pe})$ and $\bar{\rho}_{200}$ are respectively the mean density within r_{pe} and within r_{200} . Since $V^2(r) = GM(r)/r$, we can also express the ratio between the rotational velocity at r_{pe} and the asymptotic value V_{200} as

$$\left[\frac{V(r_{pe})}{V_{200}} \right]^2 = \frac{\bar{\rho}(r_{pe})}{\bar{\rho}_{200}} \left(\frac{r_{pe}}{r_{200}} \right)^2 \quad (4)$$

For a flat rotation curve, the definition of r_{pe} yields $[V(r_{pe})/V_{200}]^2 \simeq 0.4$; then

$$M(r_{pe}) \simeq 0.4 M_{200} \frac{r_{pe}}{r_{200}} \quad (5)$$

It can be shown that $r_{200} \propto M_{200}^{1/3}$; thus, for a constant value of r_{pe} :

$$M(r_{pe}) \propto M_{200}^{2/3} \quad (6)$$

Since $V_o(1 + \alpha)$ does not generally coincide with V_{200} , the effect of the luminosity dependence of α needs to be taken into account: it can be parametrized by writing $(V(r_{pe})/V_{200})^2 \propto M_{200}^\beta$, where β is small and positive. In general, Equation (6) can then be rewritten as

$$M(r_{pe}) \propto M_{200}^{2/3+\beta} \quad (7)$$

We now inquire on the dependence of the halo mass within r_{pe} on the total mass. We assume a halo density form as proposed by Navarro, Frenk & White (1997):

$$\rho_h(r) = \rho_{crit} \frac{\delta_o}{(r/r_s)(1 + r/r_s)^2} \quad (8)$$

where ρ_{crit} is the cosmological critical density, and the scaling parameters δ_o and r_s can be expressed in terms of r_{200} and a concentration index $c \equiv r_{200}/r_s$, with $\delta_o = c^3(200/3)[\ln(1+c) - c/(1+c)]^{-1}$. For small values of r , the halo mass within radius r is

$$M_h(r) = \frac{400\pi c^2 \rho_{crit} r_{200}}{\ln(1+c) - c/(1+c)} r^2 \quad (9)$$

where $M_{200} \simeq M_h(r_{200})$. For a constant r_{pe} ,

$$M_h(r_{pe}) \propto \frac{c^2}{\ln(1+c) - c/(1+c)} M_{200}^{1/3} \quad (10)$$

Numerical simulations indicate that c is mildly dependent on halo mass, *decreasing* approximately as $(M_{200})^b$ with $b \simeq -0.10$ (Navarro, Frenk & White 1997). A comparison of Equations (7) and (10) thus indicates that the mass in the halo cannot account for the inner shape of the rotation curve, unless the concentration index *increases* with halo mass, opposite to what numerical simulations suggest. An alternative interpretation is that the contribution of disk and bulge to $M(r_{pe})$ increases with galaxy luminosity (and mass), a well-exercised idea in the current literature (e.g. Burstein & Rubin 1985; Broeils 1992; Moriondo, Giovanardi & Hunt 1998; Sellwood 1999 and refs. therein). If we assume that $M(r_{pe}) = M_h(r_{pe})(1 + f_d)$, $\beta \sim 0$ and neglect the dependence of c on M_{200} ,

$$1 + f_d \propto M_{200}^{1/3}, \quad (11)$$

suggesting that as the galaxy mass increases, the fraction of baryonic material in the inner few kpc grows rather quickly. For these systems, the baryonic mass fraction may saturate at its cosmological level (i.e. these systems retain all their baryons) and their inner rotation curves may be completely determined by it.

The spirals in our sample have small bulges (they are mostly of type Sbc and Sc). Within that context, note that in an exponential disk-dominated rotation curve a rotational velocity $1 - 1/e = 0.63$ of the maximum is obtained at a radial distance of about 0.6 disk scale lengths. For galaxies in our high luminosity bin, the mean ratio between r_{pe} and the scale length of the disk light is 0.63 ± 0.02 , as shown in Table 1, while it rises to twice that value for the less luminous galaxies in our sample.

We conclude that the simplest and most likely explanation of the near constancy of $\langle r_{pe} \rangle$ among luminosity classes is that the baryonic mass fraction within the inner few kpc of spirals increases with total luminosity, and that within that region the most luminous spirals are entirely dominated by baryonic matter. We integrate photometric profiles to $r = r_{pe}$ in order to obtain I band luminosities within that radius, assuming a solar absolute magnitude of +3.94 (Livingston 2000). Estimating mass from $M(r_{pe}) = r_{pe} V(r_{pe})^2 / G$, for galaxies brighter than $M_I = -22 + 5 \log h$ we obtain a mean baryonic mass-to-light ratio $\Upsilon_I = (2.7 \pm 0.12) h \ M_\odot / L_{\odot, I}$ within r_{pe} . Individual colors for galaxies in our sample are not available; however, if we assume that spiral galaxies radiate approximately like blackbodies with $R - I \sim 0.5$, then a mean bolometric $\bar{\Upsilon} \simeq 1.25 \bar{\Upsilon}_I = 3.4 h$

M_{\odot}/L_{\odot} can be estimated. The coarse analysis presented here does not take into consideration the dynamical effect of a central bulge with a low spin parameter and we have not attempted to separate disk and bulge contributions to the light. It is interesting to compare our result with that of Bottenga (1999) for the Sb galaxy NGC 7331: from measurements of stellar velocity dispersions he obtains $\Upsilon_{I,disk} = 1.6 \pm 0.7$ and $\Upsilon_{I,bulge} = 6.8 \pm 1.0$.

5. Conclusions

We have shown that the $H\alpha/[N II]$ rotation curves of spiral galaxies exhibit a dependence of the inner slope of their rotation curves on the galaxy axial ratio. We have interpreted this result as induced by extinction occurring within disks. The effect is luminosity dependent, being stronger for the most luminous systems as previously indicated by Giovanelli *et al.* (1995) on photometric grounds.

Serendipitously, it was also found that rotation curves of galaxies of different luminosity classes exhibit approximately the same average exponential scale length in the inner regions, of about $1.7h^{-1}$ kpc (the result has potential in the determination of redshift-independent distances: we will report elsewhere on this application). This is in agreement with the idea that in the inner parts of spiral galaxies the baryonic component contributes a rapidly increasing fraction of the mass, with increasing total luminosity of systems. In fact, the most luminous galaxies in our sample appear to be completely baryon-dominated within the inner few kpc. We use this inference and the combination of spectroscopic and photometric data to estimate a mean baryonic mass-to-light ratio for that region $\bar{\Upsilon}_I = 2.7h M_{\odot}/L_{\odot,I}$ in the I band.

This work has been supported by NSF grants AST96-17069 and AST99-00695. Discussions with M. S. Roberts are thankfully acknowledged.

REFERENCES

- Bosma, A, Byun, Y., Freeman, K.C. & Athanassoula, E. 1992, ApJ 400, L21
- Bottema, R. 1999, A&A 348, 77
- Broeils, A. 1992, Ph.D. Thesis, U.of Groningen
- Burstein, D. & Rubin, V.C. 1985, ApJ 297, 423
- Calzetti, D. 2001, PASP 113, 1449
- Courteau, S. 1997, AJ 114, 2402
- Dale, D.A. & Giovanelli, R. 2000, in *Cosmic Flows 1999*, edited by S. Courteau, M. Strauss & J. Willick, ASP Conf. Ser. vol. 201, p. 25
- Davies, J.I. & Burstein, D. 1995, editors: *The Opacity of Spiral Disks*, NATO ASI Series vol. 469, Kluwer:Dordrecht
- Giovanelli, R., Haynes, M.P., Salzer, J.J., Wegner, G., da Costa, L.N. & Freudling, W. 1994, AJ 107, 2036
- Giovanelli, R., Haynes, M.P., Salzer, J.J., Wegner, G., da Costa, L.N. & Freudling, W. 1995, AJ 110, 1059
- Goad, J. & Roberts, M.S. 1981, ApJ 250, 79
- Livingston, W.C. 2000, in *Allen's Astrophysical Quantities*, ed. by A.N. Cox, Springer-Verlag:New York, p. 341
- Mathewsom, D.S. & Ford, V.L. 1996, ApJS 107, 97
- Mathewsom, D.S., Ford, V.L. & Buckhorn, M. 1992, ApJS 81, 413
- Moriondo, G., Giovanardi, C. & Hunt, L.K. 1998, A&A 339, 409
- Navarro, J.F., Frenk, C.S. & White, S.D.M. 1997, ApJ 490, 493
- Prada, F., Beckman, J.E., McKeith, C.D., Castles, J. & Greve, A. 1994, ApJ 423, L35
- Rubin, V.C., Waterman, A.H. & Kenney, J.D.P. 1999, AJ 118, 236
- Sellwood, J.A. 1999, in *Galaxy Dynamics*, ed. by D.R. Merritt, M. Valluri & J.A. Sellwood, ASP Conf. Ser. Vol. 182
- Tully, R.B., Pierce, M.J., Huang, J.S., Saunders, W., Verheijen, M. & Witchalls, P. 1998, AJ 115, 2264

Wang, J., Heckman, T.M. & Lehnert, M.D. 1997, ApJ 491, 114

Xilouris, E.M., Kylafis, N.D., Papamastorakis, J., Paleologou, E.V. & Haerendel, G. 1997, A&A 325, 135

Xilouris, E.M., Alton, P.B., Davies, J.I., Kylafis, N.D., Papamastorakis, J., & Trewella, M. 1998, A&A 331, 894

Table 1. Parameter Averages by Luminosity Class

Luminosity Range	$100 < \alpha >$	$< hr_{pe}^{\circ} >$ <i>kpc</i>	$< r_{pe}^{\circ}/r_d^{\circ} >$	$< hr_{pe}^{\circ} >_1^a$ <i>kpc</i>	$< a_{pe}^{\circ} >_1^{(a)}$ <i>arcsec</i>
$M - 5 \log h < -22.0$	-0.31 ± 0.12	1.86 ± 0.09	0.63 ± 0.02	1.90 ± 0.11	7.1 ± 0.5
$-22.0 < M - 5 \log h < -21.4$	$+0.23 \pm 0.11$	1.75 ± 0.06	0.68 ± 0.02	1.71 ± 0.06	6.2 ± 0.3
$-21.4 < M - 5 \log h < -21.0$	$+0.53 \pm 0.19$	1.73 ± 0.09	0.83 ± 0.03	1.84 ± 0.11	7.1 ± 0.5
$-21.0 < M - 5 \log h < -20.4$	$+1.64 \pm 0.17$	1.73 ± 0.08	0.95 ± 0.03	1.82 ± 0.07	7.8 ± 0.5
$-20.4 < M - 5 \log h < -19.5$	$+1.97 \pm 0.22$	1.63 ± 0.09	1.02 ± 0.04	1.85 ± 0.09	8.3 ± 0.5
$-19.5 < M - 5 \log h$	$+4.21 \pm 0.76$	1.50 ± 0.15	1.28 ± 0.08	1.94 ± 0.14	11.7 ± 0.8

^(a)Averages computed for $hr_{pe} > 1$ kpc, $a_{pe} > 3''$, distances between 20 and 80 h^{-1} Mpc, and $\log(a/b)$ less than 0.3, 0.4, 0.5, respectively for $M - 5 \log h < -21.0$, < -19.5 and > -19.5 .

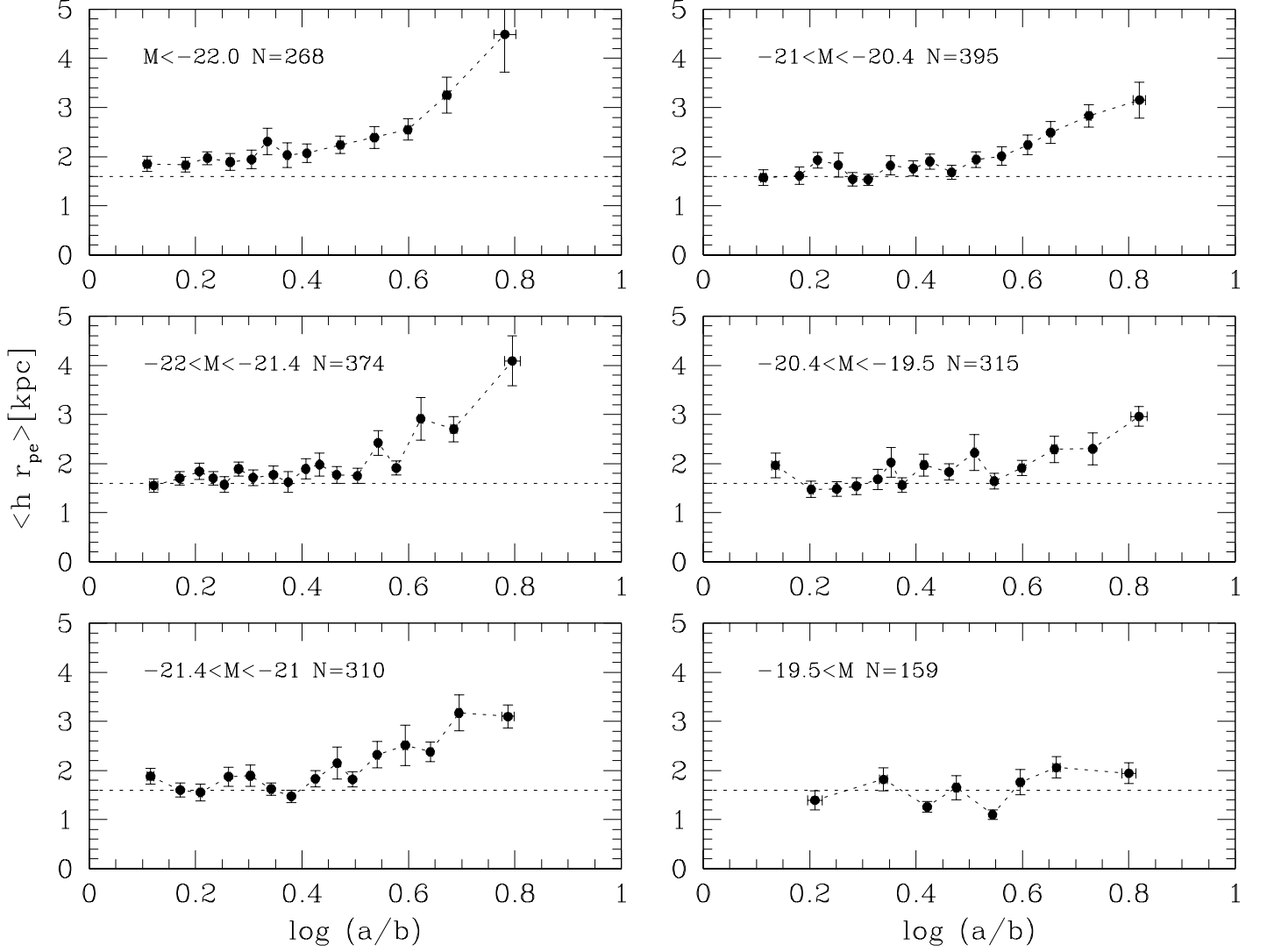


Fig. 1.— Average values of the kinematic scale length $h r_{pe}$, plotted versus $\log(a/b)$, where a/b is the galaxy’s axial ratio. Each panel displays data for the range in absolute magnitude ($M - 5 \log h$) indicated in the figure, where N is the total number of galaxies included in each panel. Systems for which r_{pe} projects at an angular size $< 3''$ have been excluded, in order to avoid angular resolution bias. The dotted line in each panel is arbitrarily drawn at a constant value of 1.6 kpc.